

# STUDY OF SPACE CHARGE EFFECTS USING A SMALL STORAGE RING THAT WORKS IN THE ISOCHRONOUS REGIME\*

F. Marti, E. Pozdeyev<sup>#</sup> and J. Rodriguez  
NSCL, MSU, East Lansing, MI 48824, USA

## Abstract

The Small Isochronous Ring (SIR) is a storage ring designed to study space charge effects in the isochronous regime. The purpose of the studies is to validate computer codes that predict space charge effects. SIR accelerates hydrogen ions and molecules to energies of approximately 20 keV. The bunches are stored for up to 200 coasting turns. With DC currents of a few tens of micro amperes we can simulate the space charge effects representative of cyclotrons like Injector 2 at PSI with significantly less power. The characteristic time scale is much longer than in the full-scale accelerators, simplifying the diagnostic equipment. We present in this paper the experimental results and comparisons with numerical calculations.

## INTRODUCTION

During the design stages of the Coupled Cyclotron Facility (CCF) [1] at Michigan State University we realized that longitudinal space charge forces on the beam would probably increase its radial extent to the point of preventing single turn extraction as we originally had envisioned. As we did not have complete confidence on the computer codes we were using, the decision was made to abandon the single turn extraction mode and assume multi-turn extraction. During this period E. Pozdeyev started as a graduate student in the accelerator group and begun developing a computer code (CYCO) to study space charge effects in isochronous machines. From the beginning the results from the code were interesting and puzzling enough that it was clear that experimental studies would be needed to validate it. We had difficulties obtaining time in the high current cyclotrons to perform accelerator physics experiments. The experimental setups would have been costly and challenging because of the power involved and short time scales. We then decided to build a small storage ring that would allow us to validate codes and perform some very basic measurements. At this point a new graduate student J. Rodriguez joined the group. All the physics design and most of the assembly has been done by the two graduate students and an undergraduate. The experiment became a very useful learning experience where the students had to deal with beam dynamics issues, magnet design, mechanical tolerances, vacuum calculations, beam diagnostics, control system, etc.

\* Work supported by NSF Grant # PHY-0110253  
# Presently at Jefferson Lab, Newport News, Va, USA

## SIR DESIGN

### Scaling laws

An important issue when studying space charge effects in cyclotrons is the difficulty in performing experiments at high current accelerators. The facilities are usually dedicated to experimental physics programs and are overbooked. The power in the beam is substantial, making it more difficult to design diagnostics probes, as well as the time scale resolution needed is very small.

It can be shown [2] that the effects of the space charge force for bunches of similar lengths approximately scale as:

$$\frac{qI}{\gamma^5 m h \omega^3}$$

where  $I$  is the total beam current,  $h$  is the harmonic number and the momentum is  $p = m\gamma R\omega$ . Taking as a point of comparison the PSI injector II cyclotron with  $I=2$  mA and SIR accelerating molecular hydrogen, we find that the equivalent *peak* current for SIR is of the order of 10  $\mu$ A, well within the reach of SIR. We can see that the SIR is approximately equivalent to the PSI Injector II from the point of view of space charge force effects.

### General layout

Several different possible configurations were explored during the design stage. Four and five sector machines were considered in the hard edge approximation. We eventually settled in the parameters shown in Table 1. A more complete description of the construction details can be found in [2-4]

Table 1: Main parameters of SIR

Beams	H <sub>2</sub> <sup>+</sup> or D <sup>+</sup>
Energy (keV)	0-30
v <sub>x</sub> , v <sub>y</sub>	1.14, 1.11
$\alpha_p$	1.0
T ( $\mu$ s)	5
Circumference (m)	6.58
I <sub>peak</sub> ( $\mu$ A)	0-100
N <sub>turns</sub>	200

The general layout of SIR can be seen in Figure 1.

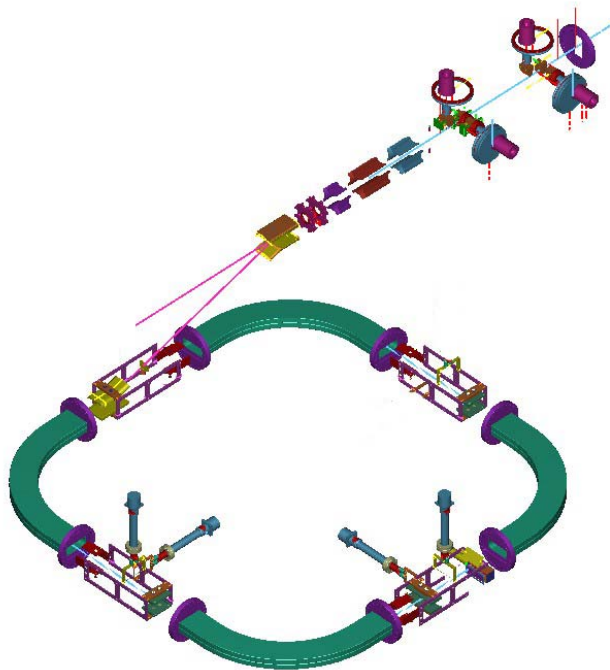


Figure 1: General layout of SIR. The four dipoles have been removed to simplify the picture. On the upper right we see the emittance measuring device followed by an electrostatic triplet, a chopper, deflection plates to deviate the beam toward the ring, and a second pair of deflection plates to inject into the median plane.

The injection into the ring is achieved by a pair of DC high voltage plates that deflect the beam from the injection line toward the ring, and a second pair of pulsed plates that bend the beam back into the median plane. The chopper in the injection line can produce bunches from about 75 ns to as long as the full ring circumference. There are four chambers in the ring. Chamber #1 is the injection chamber. In it we have the second pair of injecting plates and an electrostatic quadrupole. There is also a 3 position viewer that if fully inserted allows the detection of the beam in the injection path, or if retracted to the middle position the beam can be observed after one full turn.

Two diagnostic chambers are located at 90 and 270 degrees. They also contain electrostatic quadrupoles. There is also room for including non-intercepting capacitive pick-ups (not installed yet).

The extraction chamber is located at the 180 degrees location. The details of this chamber during assembly are shown in Figure 2. We can observe an electrostatic quadrupole, a pair of deflecting plates and a scintillator. If the deflecting plates field is reversed, the beam will be deflected downward toward a Faraday cup that is used to measure the longitudinal profile. Several versions of this cup exist, consisting of a movable single electrode or four segments, located at different radii.

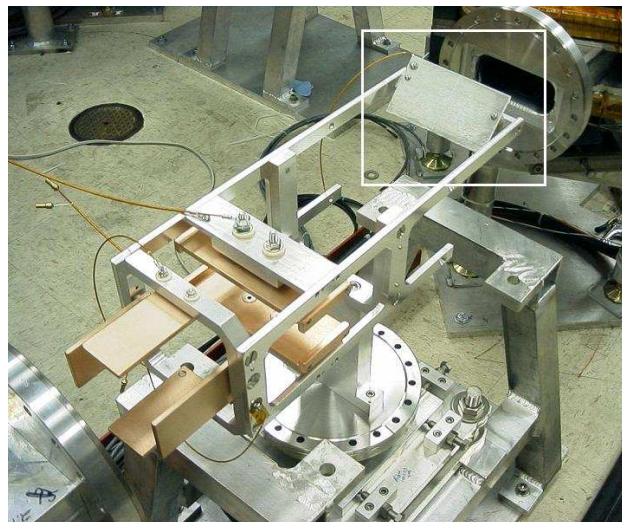


Figure 2: Extraction chamber during assembly. The deflecting plates can kick the beam up toward the scintillator (marked by the white rectangle) or down toward a Faraday cup (not shown in the photograph).

The deflecting plates are pulsed with a HV switch controlled by a variable delay generator that is synchronized to extract the beam after a variable number of turns. This same delay generator controls the chopper and the injection plates.

### Dipole magnets

The four ring dipoles have a 90° degree bending angle, a pole face angle of 26°, a gap of 71.4 mm and a pole width of 190 mm

The pole tip has been designed with edge bumps to flatten the field, see Figure 3. The field is flat within half a gauss.

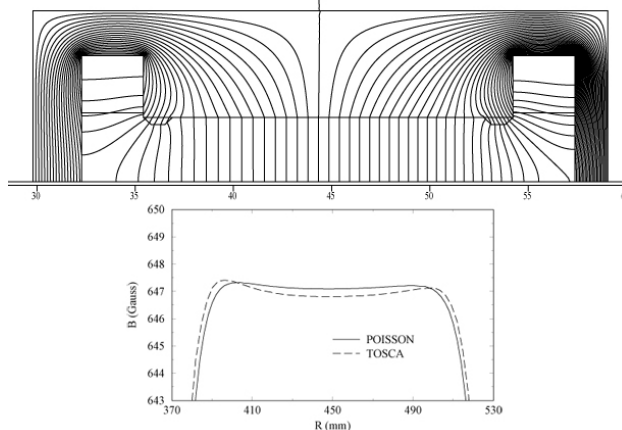


Figure 3: POISSON calculation of the SIR dipole (above) showing the edge bumps used to flatten the field. The field at the center of the magnet (below) calculated with POISSON and with TOSCA [5]. Only the top 1% of the field is displayed.

Besides the main dipole windings, we have included a correction dipole coil and a quadrupole corrector. A cut out drawing of the dipole is shown in Figure 4. The quadrupole corrector was made from an aluminum plate

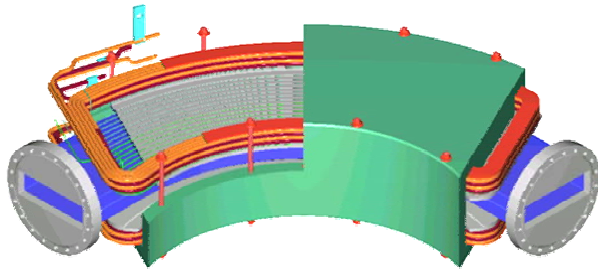


Figure 4: Cut out of the SIR dipoles.



Figure 5: Quadrupole corrector plate.



Figure 6: Photograph of the Small Isochronous Ring. The ion source is in the high voltage cage on the upper right. The extraction chamber is in the foreground. The circumference is 6.58 m.

with grooves where the insulated conductor was located. Figure 5 shows a photograph of the plate.

The ring was finished in December 2003. A photo of the ring is shown in Figure 6.

## SIMULATIONS

We have used two computer codes to calculate the beam dynamics in SIR. CYCO [6] and Warp3D [7]. Both codes predict quite well the observed behavior. Most of the simulations were performed with CYCO that was

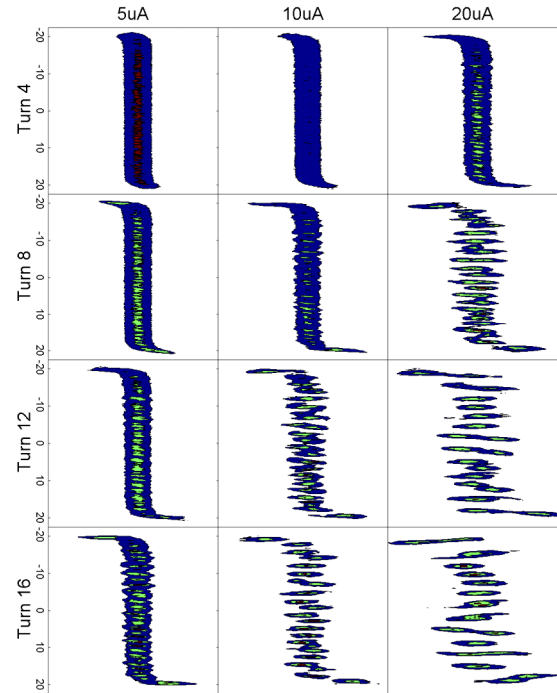


Figure 7: Results from the simulations of SIR with CYCO. Contour plots of particle density (as seen from above) is plotted for three different peak currents (5,10 and 20  $\mu\text{A}$ ) and four different turns (4, 8, 12 and 16). We see in this picture that the onset of the vortex motion as well as the fragmentation and clustering of the beam is accelerated for the higher current cases. The snapshot is taken in the straight section of SIR.

designed specifically for cyclotrons, including acceleration and neighboring turns. The codes predict the onset of the vortex motion described by M. Gordon [8]. The longitudinal space charge force increases the energy of the particles in the head of the bunch and decreases the energy of the particles in the tail. Due to the isochronous condition the head moves toward larger radii and the tail toward smaller radii. This can be observed in Figure 7 where we plot the top view of the particle density contour for three different peak currents and four different turns.

We see that the 5  $\mu\text{A}$  simulation at turn 12 seems to be at the same stage of development that the 20  $\mu\text{A}$  case is after four turns. To compare with the experimental results we should simulate the measurements made with the Faraday cup. Integrating the current in the transverse direction we obtain the plot shown in Figure 8.

The formation of a single round cluster has been predicted and observed by PSI [9]. Related effects have been seen below and above gamma transition at storage rings, where an initial longitudinal structure of the injected beam was maintained in the coasting beam due to space charge forces. See for example [10-11].



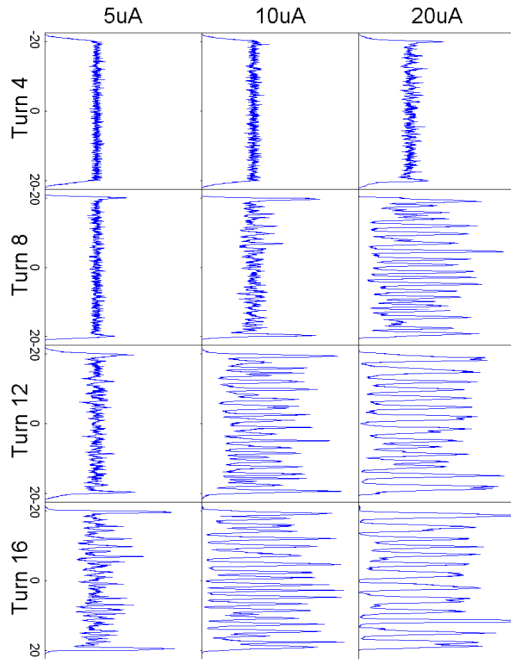


Figure 8: Longitudinal profiles of the beams and turns presented in Figure 7. These profiles simulate what the Faraday cup readings should be. They must be compared with the experimental results shown in Figure 10.

A more illustrative representation of the clustering effect can be seen in Figure 9. The current along the bunch is plotted as a function of the turn number. Starting from a uniform distribution the clusters start forming after a few turns and start coalescing around turn # 10. This representation shows more clearly that the process is less random than what Figure 8 seems to indicate. Because of rotation of the clusters around each other, two clusters can appear sometimes as a single cluster to the longitudinal probe to emerge in later turns again as two individual clusters.

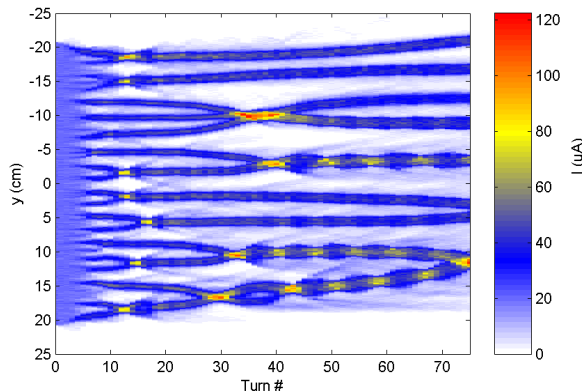


Figure 9: Current along the bunch as a function of the turn number. The clustering effect can be seen clearly. Simulations with CYCO for a 20  $\mu$ A beam.

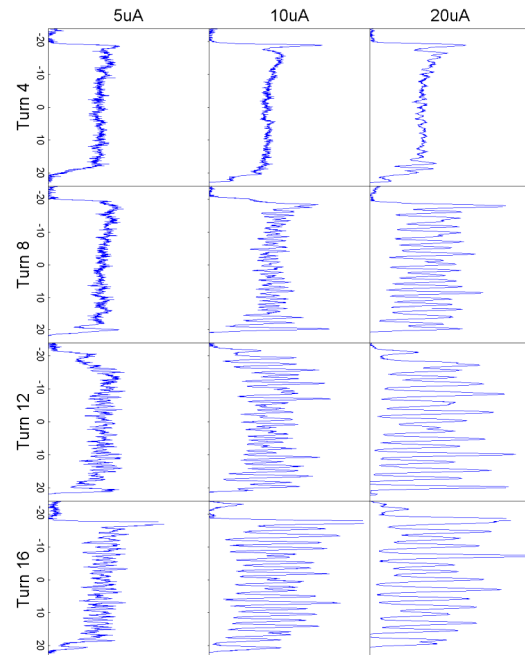


Figure 10: Experimental result from SIR for a 20 keV  $H_2^{1+}$  beam. Longitudinal profiles as measured on the Faraday cup for three different peak currents: 5, 10, and 20  $\mu$ A. Only turns 4, 8, 12 and 16 are shown

## EXPERIMENTAL DATA

The output from the segmented Faraday cup is amplified by 40 db with Miteq amplifiers AM-1607-1000. The amplified signal is recorded with a digital storage oscilloscope. Each turn is recorded for 100 consecutive bunches with a repetition time of 1 ms. A sample of the measurements is shown in Figure 10. The conditions are similar to the parameters in the simulation presented in Figures 7 and 8. It is very difficult to do detailed comparisons, because the process depends strongly on the small fluctuations of the initial beam bunch. The phase of the rotation of the clusters may line up two clusters in such a way that they look as a single group for the longitudinal probe.

An instructive comparison can be done by counting the number of clusters for each turn as seen in the longitudinal beam profiles. Figure 11 shows the number of clusters for different peak currents as a function of turn number for two different peak intensities (10 and 20  $\mu$ A). The error bars represent the  $\sigma$  of the distribution of 100 measurements. There is a significant uncertainty in counting the number of peaks because of the apparent merge of clusters in the longitudinal profile. Figure 12 shows the longitudinal beam profile for turns 0 and 99. After 99 turns we can see that the head of the tail has gained more energy than the tail and has moved to larger

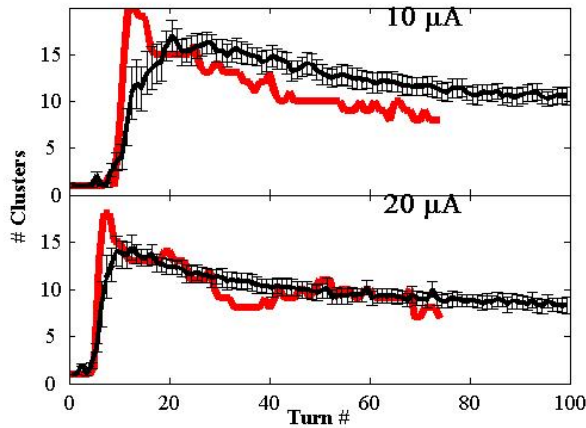


Figure 11: Comparison of the number of clusters for the simulation (solid red line) and experiment (line with error bars) for a 10  $\mu\text{A}$  (top) and 20  $\mu\text{A}$  (bottom) beam.

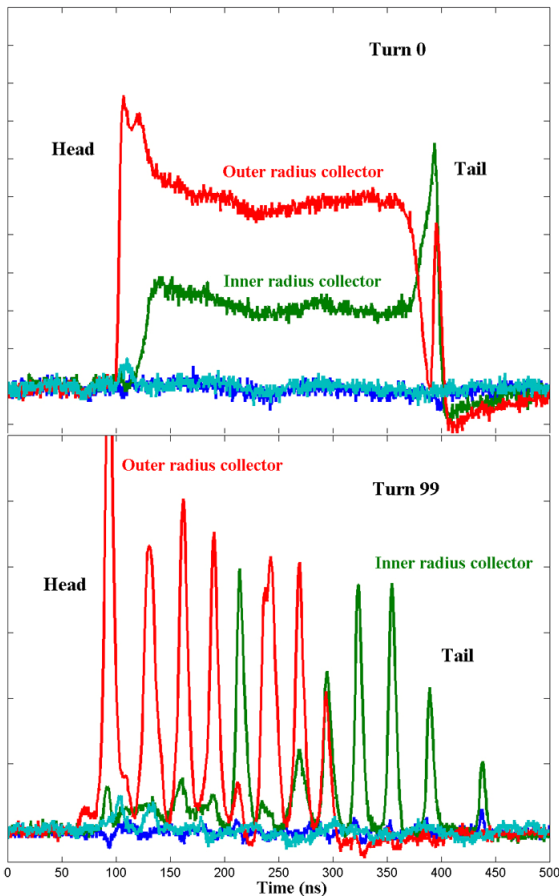


Figure 12: Longitudinal beam profiles from the segmented Faraday cup for a 10  $\mu\text{A}$ , 20.9 keV,  $\text{H}_2^{1+}$  beam. The top profile corresponds to turn 0, half a turn after injection, while the bottom one is after 99.5 turns.

radii (detected in the outer radius collector). Most of the leading clusters contribute only to the outer collector, while the tail clusters contribute mostly to the inner

collector. Some of the intermediate clusters can be seen contributing to both collectors.

## CONCLUSIONS

The experimental results from SIR agree remarkably well with the predictions from CYCO and Warp3D. The onset of the instability that breaks up the beam is described accurately by the codes. The asymptotic number of clusters observed under different conditions is also in agreement with the simulations. These verifications give us confidence to use the code CYCO to study the space charge regime in high intensity cyclotrons. Further studies are needed to understand the details of the instability.

## ACKNOWLEDGEMENTS

We would like to thank D. Deveraux, R. Fontus, D. Sanderson, R. York, A. Zeller and R. Zink for extensive help during the design and construction of SIR. We would also like to thank the personnel of the NSCL shop for their work in machining several of the SIR components, including the dipole magnets. We would also like to thank Lawrence Berkeley National Laboratory for lending us the multi-cusp source used in SIR and to D. P. Grote from LBNL for help in setting up Warp3D.

## REFERENCES

- [1] "A Coupled Cyclotron Facility at the NSCL, MSU", MSUCL-939, July 1994.
- [2] E. Pozdeyev, "CYCO and SIR: New Tools for Numerical and Experimental Studies of Space Charge Effects in the Isochronous Regime", Thesis, MSU, 2003.
- [3] J. Rodriguez, E. Pozdeyev and F. Marti, "Injection Line of the Small Isochronous Ring", EPAC'02, Paris, 2002, p. 1401.
- [4] E. Pozdeyev, F. Marti, J. Rodriguez and R. York, "Small Isochronous Ring Project at NSCL", EPAC'02, Paris, 2002, p. 1395.
- [5] Vector Fields Ltd., Oxford, England.
- [6] E. Pozdeyev and J. Rodriguez, "Computer Simulations of the Beam Dynamics in the SIR", EPAC'02, Paris, 2002, p. 1398.
- [7] D. P. Grote, A. Friedman, I. Haber, "Methods used in WARP3d, a Three-Dimensional PIC/Accelerator Code", Proc. of the 1996 Comp. Accel. Physics Conf., *AIP Conference Proceedings* **391**, p. 51 (1996).
- [8] M. M. Gordon, 5<sup>th</sup> Intl. Conference on Cyclotrons, Oxford, 1969, p. 305.
- [9] T. Stambach et al., "The PSI 2 mA Beam and Future Applications", Cyclotrons 2001, East Lansing, MI, USA, p. 423.
- [10] S. Koscielniak et al., PRST-AB vol. 4, 044201 (2001).
- [11] S. Cousineau et al., PRST-AB vol. 7, 094201 (2004).